Eur. Phys. J. B **9**, 583–592 (1999)

THE EUROPEAN PHYSICAL JOURNAL B

EDP Sciences

Nanoparticles of $Co_xFe_y\square_zO_4$: Synthesis and superparamagnetic properties

A.T. Ngo[1,2], P. Bonville[3], and M.P. Pileni[1,2,a]

[1] Laboratoire Structure et Réactivité des Systèmes Interfaciaux, Université Pierre et Marie Curie[b], B.P. 52, 4 place Jussieu, 75005 Paris, France
[2] CEA-DSM-DRECAM, Service de Chimie Moléculaire, CEA Saclay, 91191 Gif-sur-Yvette Cedex, France
[3] CEA-DSM-DRECAM, Service de Physique de l'État Condensé, CEA Saclay, 91191 Gif-sur-Yvette Cedex, France

Received 3 February 1998

Abstract. By using oil in water micelles, cobalt ferrite particles having an average diameter around 3 nm were synthetised. These nanoparticles are characterized by the presence of cation vacancies and no Fe(II) is observed, as it has been described in literature previously. Chemical interfacial treatment allows to coat the particles with citrate derivatives. The magnetic properties of uncoated and coated particles strongly diluted in a polymer substrate are compared by magnetization measurements and ^{57}Fe Mössbauer spectroscopy. The anisotropy constant is shown to be independent of coating, whereas the magnetization is found to be larger in the uncoated particles.

PACS. 75.50.Tt Fine-particle systems – 76.80.+y Mössbauer effect; other γ-ray spectroscopy – 75.30.Cr Saturation moments and magnetic susceptibilities

1 Introduction

The superparamagnetic properties of nanometric magnetic particles are an issue of current interest, both from a fundamental point of view [1] and in view of applications to materials science [2]. The change of the magnetic and structural properties induced by surface coating of the particles is also a much investigated problem [3,4]. For instance, the value of the anisotropy constant was found to change in small particles when different molecules are chemisorbed [5,6], showing that the anisotropy energy may be sensitive to surface effects.

Various methods have been developed to synthesize colloidal suspensions of nanoparticles : deposition of atomic vapours into a freezing organic solvent [7], ball milling [8], film deposition by rf sputtering [9], or coprecipitation reactions [10], which remains the most often used procedure. During the last decades, the coprecipitation reactions were carried out in aqueous solutions with a very high concentration in salt [11,12]. To obtain well defined and highly crystallized particles the solutions are heated around 65−100 °C. One of the advantages of this technique is to produce a large amount of material which is the key for technical applications. The control of the particle size is obtained by changing the base involved in the chemical reactions, the pH, etc. Because of the very different methods used to change the mean particle size, it is difficult to relate the magnetic properties to the particle size by using this technique [2,13]. Furthermore the distribution of sizes obtained by this technique is rather broad. To reduce the polydispersity, several groups use microemulsions [14,15] and vesicles [16,17], at room temperature. However the crystallinity of the material is poor and the amount of material is highly reduced. In our laboratory we recently developed a new technique by using functionalized surfactant which forms oil in water micelles [18–22]. This technique needs a rather low reactant concentration (the reactant is the counter ion of the surfactant) and the chemical reaction takes place at room temperature. The control of the mean particle size is obtained by monitoring the surfactant concentration. The surface state of the particles with different sizes can then be assumed to be the same in first approximation. The size distribution remains rather broad as with the other techniques.

In a previous work [22], we observed a change in the anisotropy of nanometric ferrimagnetic $CoFe_2O_4$ particles from cubic to axial when the mean size is reduced from 5 to 2 nm. In the present work, we concentrate on the study of $CoFe_2O_4$ particles having a mean diameter of 3 nm, which were prepared either without any chemical surface treatment (uncoated particles) or coated with citrate derivatives. Coating with citrate derivatives offers the possibility to obtain a stable magnetic fluid over a wide range of pH ($4 < pH < 10$) because of the specific adsorption of citrate anions ($NaOOC\text{-}C(OH)\text{-}(CH_2\text{-}COONa)_2$) on the ferric oxide surface [23]. These coated particles are

[a] e-mail: pileni@sri.jussieu.fr
[b] URA CNRS 1662

therefore stable in a physiological medium (pH 7) and can be used for biomedical applications [24], for instance to attach a drug molecule directly on particle surface and to reach target cells by magnetic conducting. As to the uncoated particles, they can only be dispersed in an alkaline aqueous medium with pH > 9. Previously, coating with citrate derivatives has been mainly used for controlling the particle size [25] or for size sorting [26].

The aim of the present investigation is to determine whether coating of the particles induces any change in the magnetic properties, as it has been reported by several authors [27–30], and to obtain quantitative information about the anisotropy and the saturation magnetization of the particles. For this purpose, we performed our study in samples where the particles are diluted in a polymer matrix in order to minimise magnetic interaction effects. The structural and compositional determinations were carried out using X-ray diffraction and energy dispersive spectrometry (EDS), and the magnetic properties were studied by low field magnetic measurements and by ^{57}Fe Mössbauer absorption spectroscopy in zero magnetic field and with a field of 7 T. The strong dilution of the particles allows existing single particle models to be used, at least in first approximation, in order to derive the physical quantities, but has the drawback that the signal to noise ratio is not optimal, especially for the Mössbauer study.

2 Experimental conditions and sample characterization

2.1 Products

Sodium dodecyl sulfate, Na(DS), was bought from Fluka while iron chloride $Fe(Cl)_2$, cobalt acetate, $Co(CH_3CO_2)_2$, and methylamine, CH_3NH_3OH, were purchased from Merck. Sodium citrate, $Na_3C_6O_7H_5$,$2H_2O$, tetramethylammonium hydroxide, $N(CH_3)_4OH$, and poly(vinylalcohol), $[\text{-}CH_2CH(OH)\text{-}]_n$ were produced by Aldrich whereas nitric acid, HNO_3 was from Prolabo. Cobalt and iron dodecyl sulfate, $Co(DS)_2$ and $Fe(DS)_2$, were made as described in [18].

2.2 Apparatus

A Jeol (100 kV) model JEM 100 CX II Transmission Electron Microscope was used to obtain micrographs of the cobalt ferrite particles. The energy dispersive spectrometry measurements were made with a Link AN 10,000 spectrometer. A Quanta 400 or CIA analyser was used to determine the content in Co^{2+} ions. X-ray diffraction measurements were carried out with a Stoe Stadi P goniometer and a Siemens Kristalloflex X-ray generator with a cobalt cathode driven by a personal computer through the Daco-PM interface.

The magnetometry studies were carried out in a commercial S.Q.U.I.D magnetometer with a field of 10 G between 20 K and room temperature. Both the Zero Field Cooled (ZFC) and Field Cooled (FC) procedures were used. In the ZFC measurement, the sample was cooled under zero field from 300 to 20 K; in the FC measurement, the sample was cooled in the applied field of 10 G from 300 to 20 K. In both cases, the measurements were performed on heating with, for each temperature step, a heating rate of the order of 0.5 Ks^{-1}, and a "waiting time" of approximately 100 s between the temperature stabilization and the measurement itself.

The ^{57}Fe Mössbauer absorption spectra were recorded using a $^{57}Co^*$: Rh γ-ray source mounted on an electromagnetic drive and using a triangular velocity form. Spectra were obtained in zero magnetic field in the temperature range 4.2–295 K, as well as in an external magnetic field of 7 T perpendicular to the γ-ray propagation direction at 4.2 K.

2.3 Synthesis and characterization of the samples

A mixed micellar solution composed by 5×10^{-2} M Na(DS), 4.95×10^{-3} M $Fe(DS)_2$ and 1.6×10^{-3} M $Co(DS)_2$ was kept at 30 °C. Methylamine, $[CH_3NH_3OH] = 3.8 \times 10^{-1}$ M, was added into the solution under vigorous stirring during two hours. After the appearance of a magnetic precipitate, the solid and solution phases were separated by centrifugation. Two procedures were then used:

i) The precipitate was washed with an aqueous solution of tetramethylammonium hydroxide, $N(CH_3)_4OH$ (10^{-2} M) and was redispersed in the solution. An alkaline magnetic fluid was thus obtained (uncoated particles).

ii) The precipitate was washed with HNO_3 (10^{-2} M) and then the particles were dispersed. Coating was achieved by adding sodium citrate, $[Na_3C_6O_7H_5] = 1.5 \times 10^{-2}$ M, and by stirring the solution during 30 minutes at 90 °C. Acetone was added to the solution and the particles precipitated. After washing with a large excess of acetone, the powder was dried in air and the particles coated with citrate ions were dispersed in an aqueous solution. A neutral magnetic fluid was hence obtained.

Both coated and uncoated particles show the X-ray diffraction lines of a spinel phase with a lattice constant $a = 8.41$ Å, which is consistent with that of bulk cobalt ferrite [31]. However, the X-ray diffraction peaks are too broad to allow the distinction between an inverted or a normal spinel phase.

The elemental composition determined by EDS shows 77% and 85% of iron and 23% and 15% of cobalt for uncoated and coated particles respectively. The difference in composition between coated and uncoated particles is due to the chemical treatment of the surface. Before coating, the particles have to be washed with a dilute solution of nitric acid. It is well-known that nitric acid tends to form a complex (like $Co(NO_3)_2$,$6H_2O$) [32] in aqueous solution with cobalt ions. The deficit in cobalt observed in the coated particles is due to the dissolution of cobalt ions at the particle interface *via* formation of the complex, which is removed during the chemical treatment.

The mass of cobalt ferrite in the coated particles was determined as follows: the dried powder of the sample was

dissolved in HNO_3 (2 M) at 80 °C, and the Co content was determined by a capillary ion analysis method. From the composition of the coated particles, the weight fraction of the sodium citrate in the coated particles is found to be 23%.

In order to minimize the interactions between particles, the samples were prepared by dilution of the magnetic fluid into a polyvinylic alcohol (APV) aqueous solution (1g/10 cm^3 H_2O). The weight fraction of the magnetic particles in the APV matrix is close to 1% and the mixture was dried in air, yielding rigid pellets. The presence of small particle aggregates in the APV matrix cannot in principle be discarded. However, both uncoated and coated particles bear a superficial negative charge due respectively to the adsorbed hydroxyl group and to the citrate ligands. Therefore Coulomb repulsion between particles is rather strong, which does not favour the formation of particle aggregates [23,33,34]. The estimated mean distance between isolated magnetic particles in the APV is 25 nm, *i.e.* about 8 times the average diameter.

2.4 Size distribution

The particle-size distribution was determined by Transmission Electron Microscopy (TEM) imaging. The diameter histograms, obtained with more than 500 particles, are shown in Figure 1 together with representative TEM images. The histograms are similar for uncoated and coated particles. The average diameter of both types of particles is 3.1 nm.

For the subsequent calculations, we chose to simulate the diameter distribution with a log-normal function [29,35] :

$$p(d) = \frac{1}{d\sigma_d\sqrt{2\pi}} \exp\left(-\frac{\ln^2 \frac{d}{d_0}}{2\sigma_d^2}\right) \quad (1)$$

where σ_d is the diameter standard deviation and d_0 the mean diameter. A log-normal distribution is asymmetrical, its low diameter side being steeper than its high diameter side. It is in principle adequate (and widely used) for describing the polydispersity of very small particles, where the lower particle size is usually bound for structural reasons, whereas the larger sizes can extend without such limitation. The log-normal distribution has furthermore the advantage that, if it holds for the diameters, it also holds for the volumes with a volumic standard deviation $\sigma_V = 3\sigma_d$, and a mean volume $V_0 = (\pi/6)d_0^3$. Another useful relationship is:

$$\langle V^n \rangle = V_0^n \exp\left(\frac{n^2\sigma_V^2}{2}\right). \quad (2)$$

The solid lines in Figure 1 are log-normal functions with $d_0 = 3.1$ nm and $\sigma_d = 0.25$. They reproduce the histogram shapes satisfactorily and the averages $\langle V \rangle$ and $\langle V^2 \rangle$ calculated with equation (2) are close to those obtained from the histogram weight values. Although the log-normal function may not entirely reflect the actual size distribution, it is very convenient for simulations because it yields smooth curves.

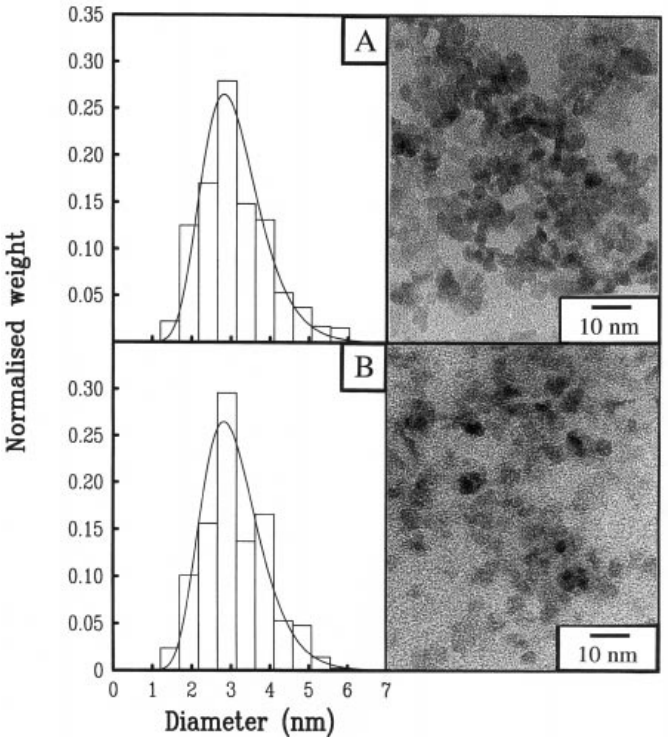

Fig. 1. Diameter histogram and TEM pattern for uncoated (A) and coated (B) Co ferrite particles made at surfactant concentration [Na(DS)] = 5×10^{-2} M, [$Fe(DS)_2$] = 4.95×10^{-3} M, $Co(DS)_2$ = 1.6×10^{-3} M, [CH_3NH_3OH] = 3.8×10^{-1} M. The solid lines on the histograms represent a log-normal distribution with $d_0 = 3.1$ nm and $\sigma_d = 0.25$.

2.5 Magnetization and ^{57}Fe Mössbauer measurements

For a ferrimagnetic particle with volume V, the magnetocrystalline anisotropy energy in axial symmetry can be expressed as:

$$E_{\text{anis}} = K\,V\,\sin^2\theta \quad (3)$$

where θ is the angle between the magnetization vector and the easy magnetic axis, and K is the magnetocrystalline anisotropy energy density. In very small particles, the anisotropy energy barrier $E_b = KV$ can be of the same magnitude as the thermal energy; then the magnetization vector can fluctuate among the easy directions of magnetization. This process is called superparamagnetic relaxation. For a single-domain particle with uniaxial anisotropy, in the absence of an applied magnetic field, the relaxation time τ at temperature T has an activation-like thermal dependence and is given by Néel's expression [36]:

$$\tau = \tau_0 \exp\left(\frac{KV}{k_B T}\right) \quad (4)$$

where τ_0 is a microscopic relaxation time, which is of the order of 10^{-10} s for ferro- or ferrimagnetic materials. This microscopic "trial" time depends in principle on the volume of the particle, on temperature and on the anisotropy

density K [37]. The blocking temperature, T_b, for a particle of volume V, is defined as the temperature for which the relaxation time τ is equal to the time scale of the given measurement technique, τ_m:

$$k_\mathrm{B}T_\mathrm{b} = \frac{KV}{\ln\left(\frac{\tau_\mathrm{m}}{\tau_0}\right)}\cdot \tag{5}$$

For an assembly of small particles with size distribution, at a given temperature, the distribution of relaxation times given by equation (4) is very broad, and extends over several orders of magnitude. As a first approximation, one may consider that the smaller particles, with a relaxation time smaller than the time scale τ_m of the measurement technique, behave as paramagnetic objects, whereas the larger ones, with τ larger than τ_m, are "blocked".

The ZFC susceptibility curve for an assembly of non-interacting small particles usually presents a maximum at a temperature T_g; at higher temperature, if the magnetization of the particle does not depend on temperature, the susceptibility falls off according to a Curie or Curie-Weiss law, representing the paramagnetic response of the rapidly fluctuating magnetization of all the particles. The reversible FC curve is expected to decrease monotonically as temperature increases and to join the ZFC curve at a temperature slightly higher than T_g. The temperature T_g of the maximum of the ZFC susceptibility is often considered as a rough estimate for a mean blocking temperature, defined by merely averaging equation (5):

$$k_\mathrm{B}\langle T_\mathrm{b}\rangle = \frac{K\langle V\rangle}{\ln\left(\frac{\tau_\chi}{\tau_0}\right)} \tag{6}$$

where $\tau_\chi \approx 100$ s is the "waiting time" characteristic of the susceptibility measurement. However, in the presence of a sizeable size distribution, it has been shown that T_g overestimates the mean blocking temperature [38,39]. A plot of the ratio $\alpha = T_\mathrm{g}/T_\mathrm{b}(V_0)$ as a function of the volumic log-normal standard deviation σ_V is given in reference [39], where V_0 is the most probable volume of the size distribution. From the T_g, V_0 and σ_V values, a first estimate of the anisotropy constant K can in principle be deduced. This procedure is however rather uncertain, and in this work, we will perform a calculation of the FC and ZFC susceptibility curves, described in Section 3, which allows a direct comparison with the experimental data to be made. The determination of the K value in this way is more correct than by using equation (6), corrected by the α value.

The qualitative features of the zero magnetic field ^{57}Fe Mössbauer spectra in nanometric particles are well-known [1]: at a given temperature, the particles with a relaxation time shorter than the ^{57}Fe hyperfine Larmor time $\tau_\mathrm{L} = 5 \times 10^{-9}$ s present a two-line hyperfine quadrupolar spectrum, whereas those with $\tau > \tau_\mathrm{L}$ present a broadened six-line magnetic hyperfine spectrum. The total spectrum is thus a superposition of a magnetic and of a quadrupolar pattern, the relative weight of the latter increasing with temperature as the number of rapidly fluctuating particles increases. One usually defines a blocking temperature T_b^M as the temperature for which half the particles are "blocked". It can serve as a first characterization for superparamagnetic Mössbauer spectra.

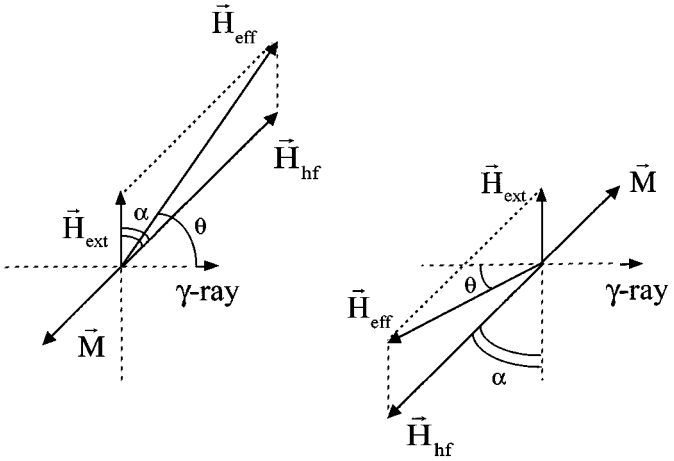

Fig. 2. Effective field $\mathbf{H}_\mathrm{eff}$ on the ^{57}Fe nucleus in the presence of an external magnetic field $\mathbf{H}_\mathrm{ext}$ for the two situations where the hyperfine field $\mathbf{H}_\mathrm{hf}$ lies in the same half-plane as $\mathbf{H}_\mathrm{ext}$ (left) or in the opposite half-plane (right). The magnetization $\mathbf{M}$ is antiparallel to $\mathbf{H}_\mathrm{hf}$ for Fe^{3+}.

In a powder sample, where the direction of the hyperfine field is at random with respect to the γ-ray direction of propagation, the intensities of the 6 lines of the magnetic hyperfine spectrum are in the ratio 3 :2 :1 :1 :2 :3. In the presence of an external magnetic field, the intensities of the 6 hyperfine lines can change if the field is sufficiently strong so as to reorient the magnetization. In a situation where the magnetization, and hence the Fe^{3+} hyperfine field, in the sample points towards a single direction, the effective field at the nucleus $\mathbf{H}_\mathrm{eff} = \mathbf{H}_\mathrm{ext} + \mathbf{H}_\mathrm{hf}$ is at an angle θ with respect to the γ-ray direction; then the line intensities, proportional to Clebsch-Gordan coefficients, have the following angular dependence:

$$\begin{cases} A_{1,6} = 3(1+\cos^2\theta) \\ A_{2,5} = 4\sin^2\theta \\ A_{3,4} = 1+\cos^2\theta \end{cases} \tag{7}$$

where $A_{i,j}$ is the intensity of line i or j (i,j = 1, 6, 2, 5 or 3, 4). The value of θ is usually obtained from the value of the ratio $r = A_{2,5}/A_{3,4}$, according to equation (7):

$$\theta = \cos^{-1}\sqrt{\frac{4-r}{4+r}}\cdot \tag{8}$$

In our experimental setup where the external field is perpendicular to the γ-ray direction, a complete alignment of the Fe^{3+} magnetization along the field direction ($\theta = 90°$) would give line intensities in the ratio 3 :4 :1 :1 :4 :3. In the case of incomplete alignment, the measurement of θ and of H_eff allows one, by a simple geometrical construction (see Fig. 2), to extract the physically interesting quantities, *i.e.* H_hf and the angle α between the hyperfine field (antiparallel to the magnetization for Fe^{3+}) and the external field.

For ferrimagnetic $CoFe_2O_4$, for a sufficiently high external field, the magnetizations of the two antiferromagnetically coupled A and B Fe^{3+} sublattices will partially reorient and thus will be pointing in opposite half-planes with respect to H_{ext}. As can be seen in Figure 2 which depicts the two possible situations, the effective fields at the ^{57}Fe nucleus are different for each magnetization orientation, and one can expect to resolve the A and B site subspectra [40].

3 Experimental results

3.1 ^{57}Fe Mössbauer measurements at room temperature

At room temperature, the Mössbauer spectra for the uncoated and coated particles show only a quadrupolar two-lines pattern with an isomer shift (with respect to α-Fe) $\delta \cong 0.34$ mm/s and a quadrupolar splitting $\Delta \cong 0.67$ mm/s, typical for Fe^{3+} ions, and show no trace of a Fe^{2+} quadrupolar spectrum. Thus, all the iron atoms are in the Fe^{3+} state in our particles. From the EDS data and the absence of detectable Fe^{2+} ions, we conclude that our Cobalt ferrites present some cationic vacancies. Taking into account the electroneutrality of the sample, uncoated and coated particles can be represented by the formulae: $Co_{0.65}Fe_{2.23}\square_{0.12}O_4$ and $Co_{0.43}Fe_{2.38}\square_{0.19}O_4$ respectively, $\square$ representing a cationic vacancy. Thus the use of functionalized surfactants enables cobalt ferrite nanoparticles having cation vacancies to be formed. To our knowledge, no cation vacancies have been observed before for samples on a nanometre scale. Furthermore, the nonstoichiometric cobalt ferrite material, $Co_xFe_{3-x}O_4$ [41–43] is well-known to have both Fe(II) and Fe(III) in the spinel structure. The nanoparticles produced by our method do not contain any Fe(II) and keep the spinel structure.

3.2 ^{57}Fe Mössbauer measurements at low temperature

We will present here the ^{57}Fe Mössbauer spectra in the uncoated particles only, between 4.2 K and 220 K (see Fig. 3). The spectra in the coated particles are of worse statistics because of the smaller quantity of available material, but they show no essential difference with respect to those of the uncoated particles.

At 4.2 K, the zero external field spectra present a slightly asymmetric 6-line hyperfine pattern, similar to that previously observed in cobalt ferrite small particles [22]. The asymmetry is due to the presence of ^{57}Fe at the A and B sites of the spinel structure with slightly different hyperfine fields. Due to the sizeable line broadening, these two sites are not resolved. The average hyperfine field for both the uncoated and coated particles is 50(1)T. On heating, the 6-line magnetic hyperfine spectra exhibit a progressive line broadening and a quadrupolar hyperfine doublet appears. A good phenomenological fit of these spectra is obtained using the superposition of a distribution of hyperfine fields (histogram) and of a quadrupolar doublet. One observes that the maximum of the hyperfine field distribution decreases as temperature increases and that the relative weight of the doublet increases. The thermal variation of the relative weight $f_p(T)$ of the doublet in the uncoated particles, representing the fraction of particles with relaxation times smaller than τ_L (superparamagnetic fraction), is shown in Figure 4. We found that f_p is stable to within a few percents with respect to small changes of the fitting procedure of the hyperfine field histogram, except at the highest temperature 220 K where the weight of the magnetic pattern is small. In Figure 4, the uncertainty is given by the size of the square symbol except at 220 K where the error bar is shown. The blocking temperature is found to be $T_b^M \approx 150$ K.

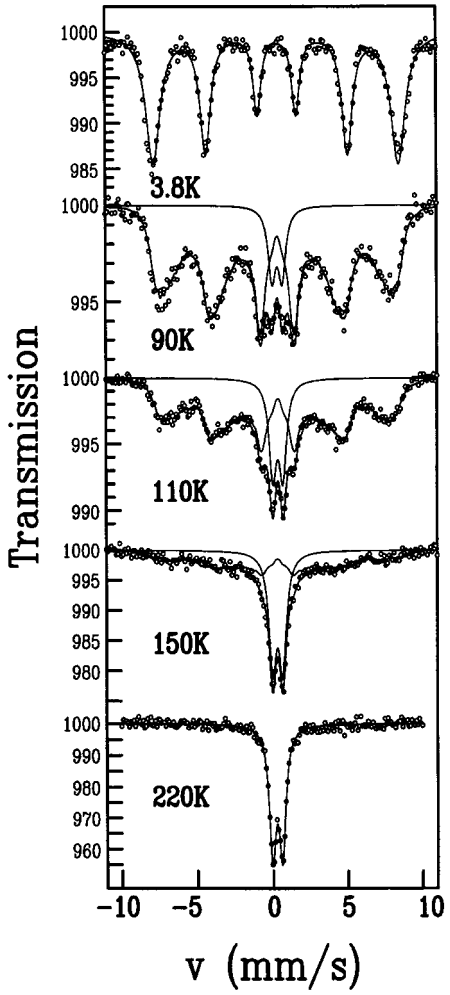

Fig. 3. ^{57}Fe Mössbauer absorption spectra in uncoated Co ferrite: particles at various temperatures between 3.8 K and 220 K in zero magnetic field. The solid lines are fits as explained in the text. The quadrupolar (rapidly fluctuating particle magnetization) and magnetic (slowly fluctuating particle magnetization) hyperfine subspectra are represented at intermediate temperatures.

At 4.2 K, the Mössbauer spectra recorded in a magnetic field of 7 T (in our experimental setup perpendicular

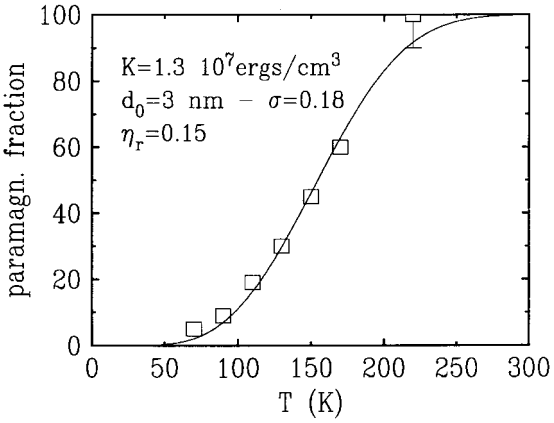

Fig. 4. Thermal variation of the percentage of the quadrupolar doublet (superparamagnetic fraction) in the ^{57}Fe Mössbauer absorption spectra of uncoated Co ferrite particles. The solid line is the calculated curve according to equation (15).

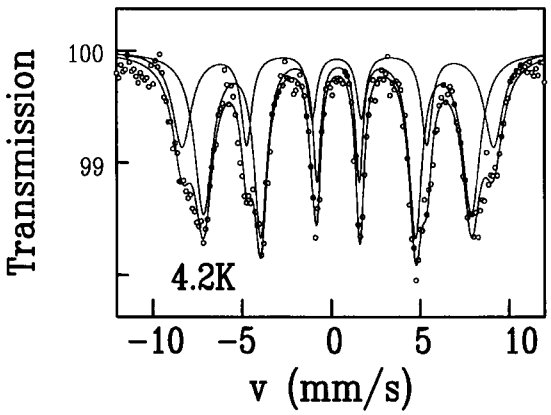

Fig. 5. ^{57}Fe Mössbauer absorption spectrum at 4.2 K in an external magnetic field of 7 T, applied perpendicular to the γ-ray direction of propagation, in uncoated Co ferrite particles. The two resolved subspectra correspond to ^{57}Fe in the A and B sites of the spinel structure.

to the propagation direction of the γ-rays) in the uncoated particles is shown in Figure 5. The spectrum is clearly resolved, with relatively narrow lines. This means that the external magnetic field has reoriented the two Fe^{3+} sublattice magnetizations in all the particles, but has not aligned them along its direction because the line intensities are clearly not in the ratio 3 :4 :1 :1 :4 :3. The spectrum was fitted with two overlapping six-line hyperfine patterns, the ratios $r = A_{2,5}/A_{3,4}$ for the two subspectra being left as free parameters. The best fit yields the following values:

(i) subspectrum 1, with 36% relative intensity: $H_{\text{eff}} = 54.2(5)$ T and $r = 1.61$, yielding $\theta = 49°$.

(ii) subspectrum 2, with 64% relative intensity: $H_{\text{eff}} = 46.7(5)$ T and $r = 2.44$, yielding $\theta = 60°$.

The modulus of the hyperfine fields and their mean tilting angles α with respect to the external field can then be determined using the geometrical construction of Figure 2, taking into account the fact that the larger effective field corresponds to a situation where the hyperfine field lies in the same half-plane as the external field. One obtains: $H_{\text{hf}} = 49.2(5)$ T and $\alpha = 46°$ for subspectrum 1, and $H_{\text{hf}} = 52.8(5)$ T and $\alpha = 26°$ for subspectrum 2. Acceptable fits can be obtained with the same hyperfine field and relative intensity values as above, but with nearly equal α values ($\approx 35°$) for both subspectra. The hyperfine field corresponding to subspectrum 1 lies in the same half-plane as the external field, and that corresponding to subspectrum 2 in the opposite half-plane. As the hyperfine field is antiparallel to the Fe^{3+} magnetization, this means that the Fe^{3+} sublattice magnetization corresponding to subspectrum 2 is in the same half-plane as the external field. Then, according to the magnetic structure of $CoFe_2O_4$, where the site B Fe^{3+} moments are parallel to the Co^{2+} moments, the external magnetic field tends to align the B site Fe and the Co moments along its direction, and we can identify subspectrum 2 (64%) with Fe ions at the B site (with $H_{\text{hf}}^{\text{B}} = 52.8$ T) and subspectrum 1 (36%) with the Fe ions at the A site (with $H_{\text{hf}}^{\text{A}} = 49.2$ T). Thus the Fe^{3+} ions are unequally distributed among the A and B sites, with an excess of Fe^{3+} ions at the B sites. In bulk $Co_{0.6}Fe_{2.4}O_4$, a similar asymmetry in the iron occupancy between A and B sites was observed [43]. The derived values of the hyperfine fields for the A and B site are compatible with the unresolved zero field hyperfine spectrum at 4.2 K.

The spectrum at 7 T in the coated particles is essentially identical to that of the uncoated particles.

3.3 Magnetic susceptibility measurements

The magnetic susceptibility curves in uncoated and coated particles are shown in Figure 6. We express the susceptibility in units of emu/cm^3 by calculating the total volume of $Co_xFe_y\square_zO_4$ material in the sample from the mass and the density obtained from the EDS and X-ray measurements (5.11 and 5.02g/cm^3 respectively for uncoated and coated particles). We have checked, for the coated particles, that the susceptibility does not depend on the weight fraction of $Co_{0.43}Fe_{2.38}\square_{0.19}O_4$ diluted in APV in a range of 1% to 0.027%. This is an indication that magnetic interaction effects between particles play a negligible role in the magnetic measurements [44]. The FC and ZFC curves for the coated particles, if scaled by a factor 1.43, almost perfectly match those of the uncoated particles. The ZFC curve presents a maximum at slightly different temperatures for the uncoated ($T_{\text{g}} = 85$ K) and coated ($T_{\text{g}} = 92$ K) particles. The irreversibility temperature at which the FC and ZFC curves coalesce is $T_{\text{irr}} \sim 130$ K. Above 150 K, in the reversible superparamagnetic regime, the susceptibility does not follow a Curie or Curie-Weiss law, as evidenced by the non-linear $\chi^{-1}(T)$ plot shown in the insert of Figure 7. The volumic susceptibility in the limit of very small field can be written, for an assembly of

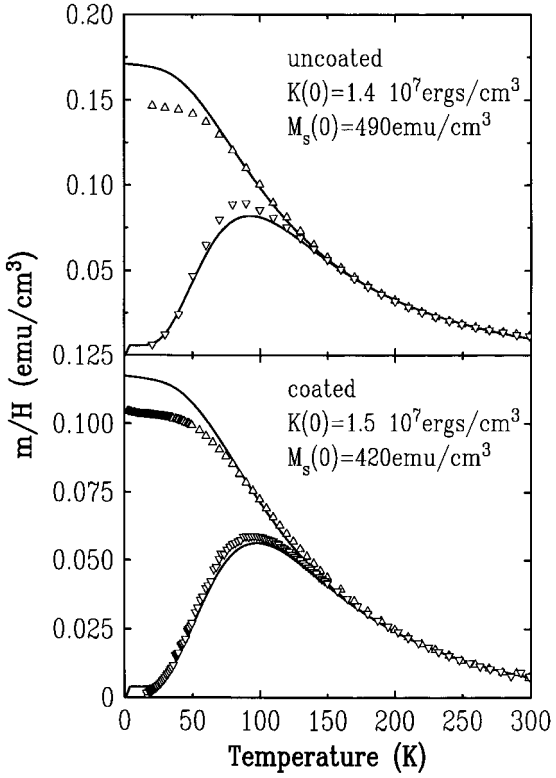

Fig. 6. ZFC (▽) and FC (△) magnetization curves with a field of 10 G in uncoated and coated Co ferrite particles. The solid lines correspond to a calculation using a model of non-interacting particles as explained in the text.

superparamagnetic small particles:

$$\chi(T) = \int_{V_{\min}}^{V_{\max}} \mathrm{d}V p(V) \frac{M_{\mathrm{s}}^2(T)}{3k_{\mathrm{B}}T} \frac{V^2}{\langle V \rangle} = \frac{M_{\mathrm{s}}^2(T)}{3k_{\mathrm{B}}T} \frac{\langle V^2 \rangle}{\langle V \rangle} \quad (9)$$

where $p(V)$ is the volume distribution function and $M_{\mathrm{s}}(T)$ is the magnetization at temperature T. The non observation of a Curie law thus may originate from a sizeable thermal dependence of the magnetization in the temperature range of the experiment. The thermal variation of $M_{\mathrm{s}}(T)$ obtained for both types of particles using equation (9), from the experimental $\chi(T)$ values and the volume averages calculated with the log-normal function, is shown in Figure 7. The dashed lines in Figure 7 represent a fit to a spin-wave type dependence of $M_{\mathrm{s}}(T)$:

$$M_{\mathrm{s}}(T) = M_{\mathrm{s}}(0)(1 - \beta T^{3/2}). \quad (10)$$

We obtain the same value for β ($10^{-4}\,\mathrm{K}^{-3/2}$) for both types of particles, and a saturation magnetization $M_{\mathrm{s}}(0)$ of 375 emu/cm^3 for the uncoated particles and 340 emu/cm^3 for the coated particles. Furthermore, a rough extrapolation of the $M_{\mathrm{s}}(T)$ curves at higher temperature suggests that the Curie temperature for our particles is of the order of 400−500 K, whereas the Curie temperature of bulk stoichiometric $CoFe_2O_4$ is close to 800 K [45].

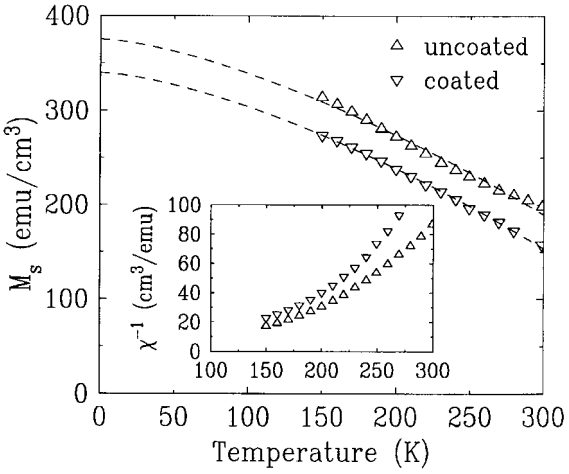

Fig. 7. Thermal variation of the magnetization (open symbols) in uncoated and coated Co ferrite particles derived from the thermal variation of the inverse susceptibility (insert). The dashed lines are fits to a spin-wave thermal dependence according to equation (10).

4 Interpretation of the results with a uniaxial anisotropy model

In order to obtain a more quantitative interpretation of the magnetic susceptibility curves, we tentatively fitted our data to a simple model explained below, assuming an anisotropy with axial symmetry, and independent spherical particles. The constancy of the susceptibility curves measured for various particle dilutions allows us to think that the latter assumption is reasonable for our particles strongly diluted in a diamagnetic medium. The assumption on the uniaxial anisotropy is more questionable, as bulk $CoFe_2O_4$ shows a magnetocrystalline anisotropy with cubic symmetry. However, our preliminary results obtained with similar nanoparticles suggest a transition from cubic to axial anisotropy with a decrease of the particle size [22]; in the 3 nm size range, the anisotropy is likely to have a dominant uniaxial character.

The model we use to compute the ZFC-FC curves is based on a distribution of blocking temperatures, as originally proposed by Gittleman [46]. For a given particle with volume V, the ZFC susceptibility is taken to be constant and equal to the frozen state random value: $\chi^{\mathrm{ZFC}} = \frac{M_{\mathrm{s}}^2 V}{3K}$ for $T < T_{\mathrm{b}}(V)$, and to follow a Curie law for $T > T_{\mathrm{b}}(V)$. For the FC curve, for $T < T_{\mathrm{b}}(V)$, the susceptibility is taken to be constant and equal to the value at $T_{\mathrm{b}}(V)$:

$$\chi^{\mathrm{FC}} = \frac{M_{\mathrm{s}}^2 V}{3k_{\mathrm{B}}T_{\mathrm{b}}(V)} = \frac{M_{\mathrm{s}}^2}{3K} \ln\left(\frac{\tau_{\mathrm{m}}}{\tau_0}\right)$$

and to follow a Curie law above $T_{\mathrm{b}}(V)$. If one defines the blocking volume $V_{\mathrm{b}}(T)$ at temperature T:

$$V_{\mathrm{b}}(T) = \frac{k_{\mathrm{B}}T}{K} \ln\left(\frac{\tau_{\mathrm{m}}}{\tau_0}\right) \quad (11)$$

then the total susceptibility is obtained by integration over the size distribution, and is given by the expressions [38,39,46] :

$$\chi^{\mathrm{ZFC}}(T) = \frac{M_{\mathrm{s}}^2(T)}{3k_{\mathrm{B}}T}\int_{V_{\min}}^{V_{\mathrm{b}}(T)} p(V)V^2\mathrm{d}V + \frac{M_{\mathrm{s}}^2(T)}{3K}\int_{V_{\mathrm{b}}(T)}^{V_{\max}} p(V)V\mathrm{d}V \quad (12)$$

$$\chi^{\mathrm{FC}}(T) = \frac{M_{\mathrm{s}}^2(T)}{3k_{\mathrm{B}}T}\int_{V_{\min}}^{V_{\mathrm{b}}(T)} p(V)V^2\mathrm{d}V + \frac{M_{\mathrm{s}}^2(T)}{3K}\ln\frac{\tau_{\mathrm{m}}}{\tau_0}\int_{V_{\mathrm{b}}(T)}^{V_{\max}} p(V)V\mathrm{d}V \quad (13)$$

where $p(V)$ is the volume distribution function taken to be a log-normal function.

The solid lines in Figure 6 represent the best fits using this model. We chose to take into account the thermal variation of the anisotropy density according to that determined in slightly nonstoichiometric $Co_{1.01}Fe_2O_{3.62}$ [47]:

$$K(T) = K(0)\exp(-1.9\times10^{-5}\,T^2) \quad (14)$$

as well as the previously determined thermal variation of the magnetization $M_{\mathrm{s}}(T)$. The thermal and volumic variation of τ_0 has been neglected, as it is not expected to play a significant role due to the dependence in ln τ_0 of the susceptibilities. We fixed $\tau_0 = 10^{-11}$ s, which is a value compatible with that obtained from the fit of the Mössbauer superparamagnetic fraction as explained below. The characteristic time of the measurement τ_χ has been taken to be 100 s, *i.e.* we define it as the average "waiting time" between the heat pulse and the measurement, which is probably a rough approximation. The free parameters in the simulations are $K(0)$, $M_{\mathrm{s}}(0)$ and the mean square deviation σ_d. The mean diameter d_0 is taken at the value 3.1 nm, as determined from the size histograms. The solid lines in Figure 6 were obtained with the common value $\sigma_d = 0.16$ for both types of particles, and with $K(0) = 1.4\times10^7$ ergs/cm^3 and $M_{\mathrm{s}}(0) = 490$ emu/cm^3 for the uncoated particles and $K(0) = 1.5\times10^7$ ergs/cm^3 and $M_{\mathrm{s}}(0) = 420$ emu/cm^3 for the coated particles. The ZFC branches as well as the irreversibility temperature are rather well reproduced, whereas the calculated FC branch saturates at a 15% too high value with respect to the experimental data. The overall agreement of the calculated FC and ZFC curves with the experimental data is however quite reasonable, taking into account the approximations inherent to our simplified model. Using the above value for $K(0)$, the most probable barrier height $E_{\mathrm{b}} = K(0)V_0$ in our Co ferrite particles is: $E_{\mathrm{b}} \cong 1585$ K.

The thermal variation of the percentage $f_{\mathrm{p}}(T)$ of the quadrupolar doublet (superparamagnetic fraction) in the Mössbauer spectra (see Fig. 4) can be obtained through the relation:

$$f_{\mathrm{p}}(T) = \int_0^{V_{\mathrm{b}}(T)} p(V)\frac{V}{\langle V\rangle}\mathrm{d}V \quad (15)$$

where $p(V)$ is the volumic distribution function and $V_{\mathrm{b}}(T)$ the blocking volume at temperature T corresponding to the Mössbauer time scale $\tau_{\mathrm{L}} = 5\times10^{-9}$ s. The microscopic time $\tau_0 \sim 10^{-10}$–10^{-11} s being of the same order of magnitude as τ_M, its temperature and volume dependence should now be taken into account in order to reproduce the thermal variation of $f_{\mathrm{p}}(T)$ with the uniaxial anisotropy model. For ferro- or ferrimagnetic materials, a theoretical expression of $\tau_0(V,T)$ has been given in reference [48]. We will use here the simplified expression given in reference [37], holding for $E_{\mathrm{b}} \geq 2.5\ k_{\mathrm{B}}T$, *i.e.* which should be valid in the temperature range of our experiments:

$$\frac{1}{\tau_0(V,T)} = \left(\frac{4}{\sqrt{\pi}}\right)\left(\frac{1.76\times10^7\,K(T)}{M_{\mathrm{s}}(0)}\right)\left(\frac{y\sqrt{y}}{y+1}\right) \times\left(\frac{1}{(1/\eta_{\mathrm{r}}) + \eta_{\mathrm{r}}\left[\frac{M_{\mathrm{s}}(T)}{M_{\mathrm{s}}(0)}\right]^2}\right). \quad (16)$$

In this expression, $y = \frac{K(T)V}{k_{\mathrm{B}}T}$ and η_{r} is a dimensionless parameter, which we assume temperature independent. We calculated the thermal variation of $f_{\mathrm{p}}(T)$ in the uncoated particles by including expression (16) for τ_0 into equation (15), and taking into account the thermal variations of $K(T)$ and of $M_{\mathrm{s}}(T)$ as above. We find that the experimental data for $f_{\mathrm{p}}(T)$ agree well with the calculation with $d_0 = 3$ nm and an anisotropy constant $K = 1.3\times10^7$ ergs/cm^3, close to that determined from the susceptibility curves; η_{r} can be taken in the range 0.08–0.25 (the solid line in Fig. 4 corresponds to $\eta_{\mathrm{r}} = 0.15$), values in agreement with those quoted for small particles in reference [37]. The width σ_d of the size distribution can be taken in the range 0.15–0.25 (the solid line in Fig. 4 corresponds to $\sigma_d = 0.18$), which is compatible with the width determined on the size histogram. The $\tau_0(V,T)$ values derived from expression (16) then range from 0.1×10^{-11} s at 50 K to 0.3×10^{-11} s at 300 K.

5 Discussion of the results

The main problem with the interpretation of our magnetization results with the above described model is that the width of the size distribution necessary to reproduce the FC and ZFC susceptibility curves ($\sigma_d = 0.16$) is markedly smaller than that derived from the fits of the size histogram to a log-normal function ($\sigma_d = 0.25$). This discrepancy can be due for one part to the approximations made for calculating the ZFC and FC curves. Indeed, the susceptibility of a particle with volume V is modelled by a kind of "step function", which is somehow unrealistic. But the discrepancy can also arise from intrinsic effects. The "width" of the calculated low temperature branch of the ZFC curve is determined by the width of the distribution of blocking temperatures $T_{\mathrm{b}}(V)$ which, according to equation (5), reflects the width of the barrier height distribution. A dependence of the anisotropy constant K

[22,49] on the particle diameter d, in $1/d$ or $1/d^2$, could narrow the distribution of the barrier heights $E_b = KV$ and thus induce a smaller effective "magnetic" σ_d value. The presence of a core which has different magnetic properties from those of the surrounding shell is sometimes invoked in studies of small particles [50–52]. We think that such a phenomenon cannot account for the smaller value of the "magnetic" σ_d, because this would cause a reduction of the "magnetic" mean diameter d_0, and we have checked that the ZFC and FC curves cannot be reproduced with a smaller d_0 value without introducing unphysically high values for the saturated magnetization $M_s(0)$. At this stage, we cannot say whether the finding of a smaller "magnetic" σ_d is a real effect or is due to the imperfection of our model.

The values of the anisotropy density $K(0)$ determined here are 1.4×10^7 ergs/cm^3 for the uncoated particles and 1.5×10^7 ergs/cm^3 for the coated particles. We think however that this difference is not significant and can be due to a slightly smaller mean diameter for the coated particles. The bulk phase $K(0)$ values determined by Schenker [47] for cobalt ferrite ($Co_{1.01}Fe_2O_{3.62}$) and that extrapolated from Iizuka and Iida [53] for $Co_{1.1}Fe_{1.9}O_4$ are 1.9×10^7 ergs/cm^3 and 1.2×10^7 ergs/cm^3 respectively. These values are close to those determined here in our $Co_xFe_y\square_zO_4$ nanoparticles, suggesting that the axial model approximation is reasonably correct and that the dominant contribution to the anisotropy is the magnetocrystalline energy. The fact that the $K(0)$ value derived from the Mössbauer data matches well that obtained from the magnetization data yields a further proof of the coherence of the model.

The volumic magnetic susceptibility of the coated particles is smaller than that of the uncoated particles by a factor 1.43. A large error in the mass of the coated particles, which is more difficult to obtain precisely, could be at the origin of this difference. However, we have checked that our determination of the mass of particles is correct within 5%. Therefore, the error on the absolute values of the susceptibility cannot exceed 5%, and the observed difference between uncoated and coated particles is a real effect, which we attribute to a larger saturation magnetization $M_s(0)$ in the uncoated particles. The $M_s(0)$ values are 375 emu/cm^3 and 340 emu/cm^3 for uncoated and coated particles respectively with $\sigma_d = 0.25$ (Fig. 7) and 490 emu/cm^3 and 420 emu/cm^3 respectively with $\sigma_d = 0.16$ (Fig. 6). The 20% larger values of the saturation magnetization obtained from the fits of the FC and ZFC curves reflect the smaller value of the "magnetic" σ_d. Estimations of the expected bulk saturation magnetization using the determined elemental composition of the particles and the ratio of Fe^{3+} ions in sites A and B, and assuming that the ions bear their full moment, yield $M_s(0) = 535(45)$ emu/cm^3 for the uncoated particles and 520(55) emu/cm^3 in the coated particles. The values measured here in the nanoparticles are smaller than the bulk estimations. The compositional difference between both types of particles can account for a small part of the difference between uncoated and coated particles, but the decrease of the magnetization with coating is likely to be a real effect, and could be due to the influence of citrate ligands attached to Fe atoms at the surface.

Concerning the behaviour of the nanoparticles in the external field of 7 T, it is of interest to compare the Zeeman and anisotropy energy scales involved. Starting with an average value $M_s(0) = 400$ emu/cm^3, one gets a mean magnetic moment of 670 μ_B per particle, and a Zeeman energy $E_Z = 3165$ K in the field of 7 T. The mean anisotropy energy per particle is $E_b = 1585$ K, which is about twice smaller than the Zeeman energy. It can therefore be qualitatively understood that the particles magnetizations, directed parallel to the B site Fe^{3+} magnetic moment, reorient close to the external field. Considering that the AF exchange field between the A and B sublattices within a particle is of the order of magnitude of a few 100 T, an external field of 7 T is not expected to induce a sizeable canting of the AF structure of the Fe^{3+} moments. Our finding of an acceptable fit of the 7 T spectrum with equal values of the tilting angles α for both A and B Fe^{3+} moments is in agreement with this consideration. However, the best fit with different values of α (26° for the B site and 46° for the A site) suggests the possibility of a slightly non-collinear AF arrangement of the Fe^{3+} moments, the angle between their directions being 160° instead of 180°. Such a non-collinear structure could arise from the observed strong unbalance between the occupations of site A and B by Fe atoms, inducing disorder in the exchange interactions.

6 Conclusion

The synthesis of cobalt ferrite magnetic fluids through a colloidal assembly is found to favor the formation of nanoparticles with cationic vacancies. ^{57}Fe Mössbauer absorption spectra and low field magnetization measurements were performed in an extended temperature range in samples where the 3 nm diameter $Co_xFe_y\square_zO_4$ nanoparticles are strongly diluted in a polymer matrix. Two types of particles were investigated: uncoated and coated with a citrate derivative. A typical superparamagnetic behaviour is observed in both types of particles. The analysis of the FC and ZFC susceptibility curves allowed us to show that a simple model of non-interacting particles reproduces the experimental data quite satisfactorily, and yields an anisotropy constant $K(0) = 1.4 \times 10^7$ ergs/cm^3 typical of Co ferrites and practically identical for uncoated and coated particles. The low field saturated magnetization is estimated around 400 emu/cm^3 and is found to be 10−20% higher in the uncoated particles. The thermal variation of the Mössbauer spectra in zero magnetic field and the spectrum in a field of 7 T are essentially identical for both types of particles. The superparamagnetic blocking temperature derived from the zero field Mössbauer spectra is $T_b^M \approx 150$ K. With a magnetic field of 7 T, we observe a partial rotation of the two antiferromagnetically coupled Fe^{3+} sublattice magnetizations towards the field direction, allowing a determination of the Fe^{3+} occupancies of the A and B sites of the spinel structure.

This study shows that coating Co ferrite particles with citrate ions does not greatly alter their magnetic properties, except for the saturated magnetization value which is found to decrease with coating. A number of previous studies [3,5,6,27,30] in small particles coated with different molecules such as acetone, oleic acid, stearic acid etc. show that coating often induces surface effects that strongly change their magnetic behavior.

An unresolved issue of our study concerns the finding of a "magnetic width" of the size distribution which is smaller than the width derived from the size histogram.

We are grateful to thank Dr. G. Lebras and E. Vincent from the Service de Physique de l'État Condensé (Saclay) for their help with the SQUID measurements.

References

1. J.L. Dormann, D. Fiorani, E. Tronc, *Advances in Chemical Physics* (Prigogine and Rice, 1997),Vol. XCVIII, p. 283.
2. A.H. Morrish, in *Studies of Magnetic properties of fine particles and their Relevance to Materials Science*, edited by J.L. Dormann, D. Fiorani (Elsevier Sciences Publisher, Oxford, 1992), p. 181.
3. P.V. Hendriksen, C.A. Oxborrow, S. Linderoth, S. Morup, M. Hanson, C. Johansson, F. Bodker, K. Davies, S.W. Charles, S. Wells, Nucl. Instr. Meth. Phys. Res. B **76**, 138 (1993).
4. A.E. Berkowitz, J.A. Lahut, C.E. VanBuren, IEEE. Trans. Magn. **16**, 184 (1980).
5. S. Morup, H. Topsoe, J. Lipka, J. Phys. Colloq. France **37**, C6-287 (1976).
6. E. Tronc, J.P. Jolivet, Hyperfine Interac. **28**, 525 (1986).
7. K.A. Eason, K.J. Klabunde, C.M. Sorensen, *Polyhedron* (Elsevier Science, Ltd, 1994), Vol. 13, p. 1187.
8. J. Ding, T. Reynolds, W.F. Miao, P.G. Mc Cormick, R. Street, Appl. Phys. Lett. **65**, 3135 (1994).
9. S. Koutani, G. Gavoille, J. Magn. Magn. Mater. **138**, 237 (1994).
10. W.C. Elmore, Phys. Rev. **54**, 309 (1938).
11. H. Tamura, E. Matijevic, J. Colloid Int. Sci. **90**, 100 (1982).
12. S.W. Charles, J. Popplewell, *Ferromagnetic Materials* (North-Holland Publishing Company, Amsterdam, New York, Oxford, 1982), Vol. 2.
13. T. Shinjo, J. Phys. **3**, 6 (1979).
14. J.P. Chen, C.M. Sorensen, K.J. Klabunde, G.C. Hadjipanayis, J. Appl. Phys. **76**, 6316 (1994).
15. V. Chhabra, P. Ayyub, S. Chattopadhyay, A.N. Maitra, Mat. Lett. **26**, 21 (1996).
16. I.I. Yaacob, S. Bhandarkar, A. Bose, J. Mater. Res. **8**, 573 (1993).
17. I.I. Yaacob, A.C. Nunes, A. Bose, D.O. Shah, J. Colloid Int. Sci. **168**, 289 (1994).
18. N. Moumen, P. Veillet, M.P. Pileni, J. Magn. Magn. Mater. **149**, 67 (1995).
19. N. Moumen, M.P. Pileni, J. Phys. Chem. **100**, 1867 (1996).
20. N. Moumen, M.P. Pileni, Chem. Mater. **8**, 1128 (1996).
21. N. Feltin, M.P. Pileni, Langmuir **13**, 3927 (1997).
22. N. Moumen, P. Bonville, M.P. Pileni, J. Phys. Chem. **100**, 14410 (1996).
23. J.C. Bacri, R. Perzynski, D. Salin, V. Cabuil, R. Massart, J. Magn. Magn. Mater. **85**, 27 (1990).
24. J.C. Bacri, R. Perzynski, D. Salin, La Recherche, Vol. 18, n°192 (1987), p. 1150.
25. A. Bee, R. Massart, S. Neveu, J. Magn. Magn. Mater. **149**, 6 (1995).
26. R. Massart, E. Dubois, V. Cabuil, E. Hasmonay, J. Magn. Magn. Mater. **149**, 1 (1995).
27. S. Morup, J. Magn. Magn. Mater. **49**, 45 (1983).
28. A.E. Berkowitz, J.A. Lahut, I.S. Jacobs, L.M. Levinson, D.W. Forester, Phys. Rev. Lett. **34**, 594 (1975).
29. R. Kaiser, G. Miskolczy, J. Appl. Phys. **41**, 1064 (1970).
30. S. Morup, H. Topsoe, B.S. Clausen, Phys. Scr. **25**, 713 (1982).
31. J. Smit, H.P.J. Wijn, Advan. Electron. Electron. Phys. **6**, 83 (1954).
32. R.S. Young, *Cobalt Its Chemistry, metallurgy, and uses* (American Chemical Society. Monograph Series), Vol. 149, p. 77.
33. R. Massart, IEEE Trans. Magn. **17**, 1247 (1981).
34. O. Jarjayes, P.H. Fries, G. Bidan, J. Magn. Magn. Mater. **137**, 205 (1994).
35. C.G. Granquist, R.A. Buhrmann, J. Appl. Phys. **47**, 2200 (1976).
36. L. Néel, Ann. Geophys. **5**, 99 (1949).
37. E. Tronc, Nuovo Cim. D **18**, 163 (1996).
38. C. Johansson, M. Hanson, P.V. Hendriksen, S. Morup, J. Magn. Magn. Mater. **122**, 125 (1993).
39. R. Sappey, E. Vincent, N. Hadacek, F. Chaput, J.P. Boilot, D. Zins, Phys. Rev. B **56**, 14551 (1997).
40. J. Chappert, R.B. Frankel, Phys. Rev. Lett. **19**, 570 (1967).
41. H. Franke, M. Rosenberg, J. Magn. Magn. Mater. **4**, 186 (1977).
42. T.L. Templeton, A.S. Arrott, A.E. Curzon, A.A. Gee, X.Z. Li, Y. Yoshida, P.J. Schurer, J.L. LaCombe, J. Appl. Phys. **73**, 6728 (1993).
43. Dong Hoon Lee, Hong Seok Kim, Jeong Yong Lee, Chul Hyun Yo, Keu Hong Kim, Solid State Commun. **96**, 445 (1995).
44. T. Jonsson, J. Mattsson, C. Djurberg, F.A. Khan, P. Nordblad, P. Svedlindh, Phys. Rev. Lett. **75**, 4138 (1995).
45. G.A. Sawatsky, F. van der Woude, A.H. Morrish, J. Appl. Phys. **39**, 1204 (1968).
46. J.I. Gittleman, B. Abeles, S. Bozowski, Phys. Rev. B **9**, 3891 (1974).
47. H. Schencker, Phys. Rev. **107**, 1246 (1957).
48. W.T. Coffey, D.S.F. Crothers, Yu.P. Kalmykov, E.S. Massawe, J.T. Waldron, Phys. Rev. E **49**, 1869 (1994).
49. H. Hanson, C. Johansson, M.S. Pedersen, S. Morup, J. Phys-Cond. **7**, 9269 (1995).
50. J.M.D. Coey, Phys. Rev. Lett. **27**, 1140 (1971).
51. K. Haneda, CAN. J. Phys. **65**, 1233 (1987).
52. A.H. Morrish, K. Haneda, J. Appl. Phys. **52**, 2496 (1981).
53. T. Iizuka, S. Iida, J. Phys. Soc. Jap. **21**, 222 (1966).